JPRS 78855

28 August 1981

China Report

SCIENCE AND TECHNOLOGY

No. 122

FBIS FOREIGN BROADCAST INFORMATION SERVICE

NOTE

JPRS publications contain information primarily from foreign newspapers, periodicals and books, but also from news agency transmissions and broadcasts. Materials from foreign-language sources are translated; those from English-language sources are transcribed or reprinted, with the original phrasing and other characteristics retained.

Headlines, editorial reports, and material enclosed in brackets [] are supplied by JPRS. Processing indicators such as [Text] or [Excerpt] in the first line of each item, or following the last line of a brief, indicate how the original information was processed. Where no processing indicator is given, the information was summarized or extracted.

Unfamiliar names rendered phonetically or transliterated are enclosed in parentheses. Words or names preceded by a question mark and enclosed in parentheses were not clear in the original but have been supplied as appropriate in context. Other unattributed parenthetical notes within the body of an item originate with the source. Times within items are as given by source.

The contents of this publication in no way represent the policies, views or attitudes of the U.S. Government.

PROCUREMENT OF PUBLICATIONS

JPRS publications may be ordered from the National Technical Information Service, Springfield, Virginia 22161. In ordering, it is recommended that the JPRS number, title, date and author, if applicable, of publication be cited.

Current JPRS publications are announced in Government Reports Announcements issued semi-monthly by the National Technical Information Service, and are listed in the Monthly Catalog of U.S. Government Publications issued by the Superintendent of Documents, U.S. Government Printing Office, Washington, D.C. 20402.

Indexes to this report (by keyword, author, personal names, title and series) are available from Bell & Howell, Old Mansfield Road, Wooster, Ohio 44691.

Correspondence pertaining to matters other than procurement may be addressed to Joint Publications Research Service, 1000 North Glebe Road, Arlington, Virginia 22201.

JPRS 78855

28 August 1981

CHINA REPORT
SCIENCE AND TECHNOLOGY
No. 122

CONTENTS

PEOPLE'S REPUBLIC OF CHINA

NATIONAL DEVELOPMENTS

Oceanographic Survey Ship Launched
(SHAANXI RIBAO, 20 Jul 81).. 1

APPLIED SCIENCES

Nanjing Fiber Optic Communications Line Tested
(DIANLI JISHU, 5 Apr 81).. 2

Paper on Recoverable Earth-Oriented Technology Satellites
(Yang Jiachi, et al.; YUHANG XUEBAO, Jan 81).................... 9

Briefs

Large Capacity Desalination Complex 30

ABSTRACTS

CEMENT PRODUCTION

SHUINI [CEMENT], No 7, 1981.. 31

CONSTRUCTION

JIANZHU [BUILDING CONSTRUCTION], No 6, 30 Jun 81...................... 32

ELECTRIC POWER

DIANLI JISHU [ELECTRIC POWER], No 6, 5 Jun 81........................ 34

ELECTRONICS

DIANSHIJIE [ELECTRICAL WORLD], No 6, 1981.............................. 36

MEDICAL RESEARCH

YICHUAN [HEREDITAS], No 4, Jul 81...................................... 37

RESEARCH

XIANDAIHUA [MODERNIZATION], No 7, 16 Jul 81........................... 39

OCEANOGRAPHIC SURVEY SHIP LAUNCHED

Xian SHAANXI RIBAO in Chinese 20 Jul 81 p 4

[Text] The Chinese designed and built marine geophysics survey ship, "the Kexue No 1", was recently delivered for trial voyage by the Chinese Academy of Sciences Oceanography Institute and will conduct a multidisciplinary survey in the East China Sea. "The Kexue No 1" survey ship was built by the Hudong Shipyard in Shanghai and is equipped with imported advanced satellite navigation, position finding and seismologic equipment. It can conduct studies in marine geophysics, marine geology, hydrology, meteorology, chemistry and biology.

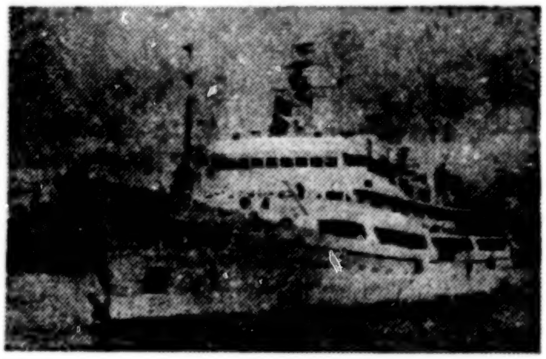

"The Kexue No 1" survey ship leaving port.

CSO: 4008/452

APPLIED SCIENCES

NANJING FIBER OPTIC COMMUNICATIONS LINE TESTED

Beijing DIANLI JISHU [ELECTRIC POWER] in Chinese No 4, 5 Apr 81 pp 34-36

[Article by the Communications Research Laboratory of the Nanjing Automation Institute: "Nanjing Fiber Optic Communications Test Line"]

[Text] I. General Situation

Fiber optic communications is a new type of communications method that has emerged in the field of communications. It has a large communications capacity, strong resistance against electromagnetic interference, small transmission loss, it is convenient to install, and it can save a large amount of ferrous metals. In recent years, it has been noticed by the advanced nations. According to reports, there are at least several hundred organizations in the world engaged in fiber optic communications. At present, fiber optic communications technology has already stepped out of the laboratory and has entered into the phase of comprehensive testing. There are over 100 fiber optic communications lines in the world now being tested and operated. Our nation's fiber optic communications research began relatively late but progress has been fast. At present, our nation's postal and telcommunications and railroad departments have established testing of fiber optic communications. Becuase optical fibers can insulate themselves from electromagnetism, the superiority of fiber optic communications is more visible in applications in electric power systems. Some nations have first applied fiber optic communications in electric power systems, and even wrapped fiber optic cables with electric power cables to transmit various kinds of control information.

To utilize fiber optic communications in our nation's electric power system, the Nanjing Automation Institute of the Ministry of Electric Power established a fiber optic communications staff at the end of 1977 and began to study the application of fiber optics in electric power systems. In November, 1978, the laboratory used a 20-meter optical fiber to transmit television images. In 1979, an optical terminal was developed for the fiber optic communications test line from the Nanjing Power Supply Bureau to the Midtown Transformer Staton and the technical problems of optical fiber coupling was solved. On 1 October of the same year, a 500-meter optical fiber was used in the laboratory to transmit television images and PCM pulse coded messages. In December, the laboratory again used a 1.8-kilometer optical cable to transmit analog television images and telephone communications. In January of 1980 under the cooperation of the Nanjing Power Supply Bureau, the first fiber optic communications test line of the electric power system was established from the Nanjing Power Supply Bureau to the Midtown Transformer Station. It successfully transmitted dispatched telephone communications, telemechanic signals and television images.

This experimental line is 1.8 kilometers long, 600 meters of the line are supported on the same pole as a 10 kilovolt high voltage power line. The optical cable hangs on a fixed iron line and is strung along the iron line at varying distances in between with large gaps of 50 meters and small gaps of 30 meters. This is our nation's first suspended optical cable test line.

The Nanjing Power Supply Bureau was in charge of setting up this optical cable. Because the optical cable has fixed connections, therefore during installation, the positions of the fixed connections were determined first then the cable was installed from the center outward in two directions. To prevent too much pull on the optical cable, during installation, a guide pulley was hung on each pole and at corners. The weight of the optical cable was lighter than electrical cable, installation was convenient, and this optical cable was completely installed within one day.

The components used by this test line were all domestically produced. The optical cable was provided by the Shanghai Electrical Cable Institute and the Shanghai Xinhu Glass Plant. The emitting diode was provided by the Shanghai Metallurgical Institute of the Chinese Academy of Sciences and the 519 Plant of the Postal and Telecommunications Ministry. The PIN probe was provided by the 519 Plant of the Ministry of Posts and Telecommunications.

II. Major Performance Indicators

1. Transmission distance. A distance of 1.8 kilometers (consisting of two optical cables of 960 meters and 840 meters long connected by a fixed connection).

2. Optical cable. The optical cable has four core optical fibers, (multiple mode grdient type, diameter of 60/150 micrometers), one pair of power lines of 0.5 millimeter in diameter, one fortification core.

3. Optical cable loss

(1) The Shanghai Electrical Cable Institute measured the loss with a direct current light signal through a bypass (stable condition) under a room temperature of +18° C, the values are listed in Table 1.

Table 1

光纤序号 1 损 2 耗 光注入端 3	1	2	3	4
A—B	3.27	3.07	2.87	4.12
B—A	2.97	3.6	3.13	4.81

注：A—B端是指光从960米段光缆通向840米段光缆。

4 B—A端是指光从840米段光缆通向960米段光缆。

Key:

1. Number of optical fiber
2. Loss
3. Light signal input end
4. Note: A-B refers to the light signal entering the 960-meter segment and traveling towards the 840-meter segment.
   B-A refers to the light signal entering the 840-meter segment and traveling towards the 960-meter segment.

(2) The loss was used to test the line and then an LED light source was used to measure the loss without going through the bypass (unstable condition), the values are listed in Table 2.

Table 2

1 光纤序号	2 光注入端	3 直流光衰耗（分贝/公里）	4 交流光衰耗（分贝/公里）
1	A—B	8.33	4.44
2	B—A	8.33	4.44
3	A—B	5.27	4.22

5注：4号光纤作为备用，没有测试。

Key:

1. Number of optical fiber
2. Light input end
3. Direct current light loss (decibel/kilometer)
4. Alternating current light loss (decibel/kilometer)
5. Note: No 4 optical fiber served as backup and was not tested.

4. Method of Regulation

Simulated signals were used directly for regulation.

5. Information Transmission

(1) A single channel black and white television image, frequency band width of 0 - 8 megahertz.

(2) Transmitting 250 baud telemechanically, there were remote test signals, remote communications signals and remote control signals.

(3) Transmitting carrier wave telephone communication, carrier wave frequency was 272 - 276 kilohertz and 352 - 356 kilohertz.

6. Optical terminal and electrical terminal interface

Input, output range: 1 $V_{\text{peak - peak}}$

Input, output impedance: 75 ohms (not balanced).

7. Optical output terminal

Light source: LED gallium arsenide diisomer luminous diode.

Optical wavelength: 0.83 micrometers.

Method of connection with the optical cable: There is a movable connector and there is also a fixed connection.

The power of alternating light of the output (including optical fiber output) light power transmission of television image was 39.8 microwatts (-14 milliwatt decibel), the power of alternating light for telephone transmission was 0.933 microwatt (-30.3 milliwatt decibel).

8. Light input terminal

Probe: PIN silicon photoelectric diode, photoelectric conversion efficiency of 0.4 microampere/microwatt, lowest receiving electrical potential of -38 milliwatt decibel, response rate < 5 millimicroseconds.

Method of connection with the optical cable: Fixed connection.

Sensitivity of optical receiver: The power of alternating light for reception of television image was 0.31 microwatt (-35 milliwatt decibel), the power of alternating light for telemechanic reception of telephone communication was 0.11 microwatt (-39.23 milliwatt decibel).

9. Power source

Input voltage: ~ 220 volts.

Output voltage: ±12 volts, ±6 volts.

Power loss: about 5 watts.

III. Telemechanic Principles of Transmitting Television Images and Telephone Communications

The transmission system (see diagram below) of this fiber optic communications test line uses the analog type. The analog electrical signal directly regulates the LED emitting diode for photoelectric conversion into light signals. The advantage of this type of transmission of light waves through the light guiding fiber is that the equipment is simple and reliable, it can be conveniently connected to the presently available communications equipment of the electric power system (the communications equipment used in our nation's electric power system is mostly analog).

Illustration of the fiber optic communications transmission system

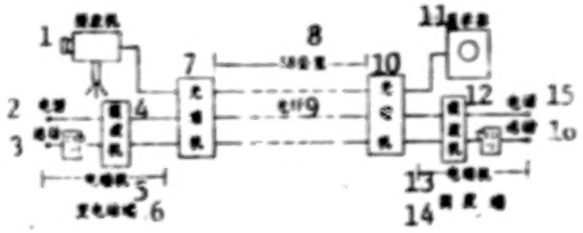

Key:
1. Camera
2. Telephone
3. Telemechanic device
4. Carrier wave generator
5. Electrical terminal
6. Transformer station terminal
7. Optical terminal
8. 1.8 kilometers
9. Optical fiber
10. Optical terminal
11. Display screen
12. Carrier wave generator
13. Electrical terminal
14. Regulator terminal
15. Telephone
16. Telemechanic device

This test line transmits television images using a fixed focal distance and a single camera installed at the transformer station. A 19-inch color television is converted to serve as a display screen installed at the regulator terminal forming a monitoring system. It can monitor the operation of the high voltage switch, the transformer and other equipment in the transformer station, and the personnel on duty in the main control room.

Transmission of telephone communications and telemechanic signals uses the ZZD-5 model electrically powered carrier wave generator, the TSY-2 model digital telemechanic device and the JYD-1 model sound frequency channel equipment connected all together forming a remote regulatory telephonic monitoring system with 20-point remote control, 28-point remote signaling, 28-point remote testing of signals.

In the entire fiber optic communications transmission system, the television image, the telephone and telemechanic transmission are transmitted via different optical fibers in a single optical cable. One optical fiber transmits the television image signals, the second optical fiber transmits telephone and telemechanic signals. In this way, one optical fiber corresponds to one light source and one optical probe, therefore on the optical terminal at the transformer station are installed two light emission dishes and one light receiving dish. One is used to send television images, the other is used to send telephone and telemechanic signals. On the regulator terminal's optical terminal is installed a light emission dish and two light receiving dishes. The emitting dish is used to transmit telephone and telemechanic signals. The ZDD-5 model electrically powered carrier wave generator can be used for repeated telemechanic transmission, the telephone and the telemechanic signals use the same optical fiber for transmission. Here, the ZDD-5 model electrically powered carrier wave generator must be changed to four high frequency lines to separate reception and transmission. Transmission to the opposite terminal is realized via the transmission brnach channel of the carrier wave generator through the alternator which is connected to the optical terminal's transmission dish by converting the electrical signal to a light signal and sending it into the optical fiber. The telephone and telemechanic light signals transmitted via the other optical fiber enter the light receiving dish of the optical terminal and the light signals of the telephone and telemechanic transmission are converted to electrical signals and sent to the signal receiving branch channel of the carrier wave generator, thus forming a channel for the transmission of telephone and telemechanic signals.

IV. Results of Establishing the Fiber Optic Communications Test Line

1. The fiber optic communications test line has transmitted television images and telephone and telemechanic information. The test results show that the television image is clear, the sound of telephone transmission is clear, and telemechanic signals are accurate and reliable. The dispatcher can view the main transformer in the Midtown transformer station directly on the television screen in the dispatcher room, the state of the switches and the personnel on duty. The results of using fiber optic communications to transmit regulatory commands and to carry out remote testing, remote signaling and remote control are good.

2. By testing the line, we proved that fiber optic communications can resist strong electromagnetic interference. This optical cable was set up on the same pole with a 10 kilovolt high voltage power line. The efficiency value of the power frequency sensitive voltage (cable - ground voltage) on the dynamic curve measured in the optical cable (ϕ 0.5 millimeter copper wire) was 16 volts while the fiber optic communications did not receive any interference.

3. Optical fibers are insulating materials, they are not affected by electromagnetic fields. Optical cables set up on the same pole with high voltage power lines can be directly installed into the dispatcher station and the transformer station or the carrier wave generator room of the power plant without the need for damping devices, coupled capacitors, connecting wave filters, and this saves investment and improves reliability of communications.

4. Through testing, we further grasped the variation of attenuation in the domestically produced optical equipment and optical cables. We discovered tha the output light power of the LED emitting diode dropped more, and using the same light power meter for measurements, we found that when the test line was first installed, the measured driving electrical current was 90 millamperes, the output light power was 49 microwatts, after half a year, the measured driving electrical current was 90 millamperes, the output light power was 37.5 microwatts. The attenuation in the optical cable of the test line varied minutely with changes in weather and temperature.

5. We also utilized the test line to perform the following tests:

(1) We used the error code rate tester to transmit AMI codes and HDB_3 codes of the PCM pulse code messages and measured an error code rate of less than 10^{-9}.

(2) We used two optical fibers connected together and successfully transmitted television images via 3.6 kilometers.

6. The test line shows the operation of the optical terminal is reliable, and operation is simple. At the time, the transformer station was undergoing expansion and construction was being carried out, there was a lot of dust, but the optical terminal could adapt to the relatively poor working environment, it was switched on and off frequently and it did not need readjustment and it could operate normally.

7. After completion of this fiber optic communications test line, many tentative ideas by communications workers of the electrical power system have emerged: The use of fiber optic communications has a large capacity, the resistance to interference is strong, and installing optical cables on the same pole as power lines or on suspended ground power lines can solve the problem of transmitting telemechanic information from the transformer station and the communications center station (switchboard) and dispatching telephone calls into urban areas at once.

9296
CSO: 4008/416

PAPER ON RECOVERABLE EARTH-ORIENTED TECHNOLOGY SATELLITES

Beijing YUHANG XUEBAO [JOURNAL OF THE CHINESE SOCIETY OF ASTRONAUTICS] in Chinese No 1, Jan 81 pp 1-13

[Article by Yang Jiachi [2799 0857 1062], Zhang Guofu [1728 0948 1381], Sun Chengqi [1327 2110 0796], Feng Xueyi [7458 1331 5030], and Niu Yinsheng [6873 1377 3932]

I Introduction

The first generation three-axis stabilized attitude control system was used on China's recoverable earth-oriented technology satellites and successfully completed its design missions, which are: 1) to eliminate the initial attitude bias caused by separation of the carrier vehicle and the satellite; 2) to meet the precision requirements of satellite attitude and angular velocity during orbit; and 3) to allow rapid changes of satellite attitude about the pitch axis for re-entry.

In this paper, the composition and main function of the attitude control system are introduced and considerations for selecting the key system parameters are discussed. In addition, an analysis of the flight test results is also presented.

II Description of the Attitude Control System and Considerations for Selecting the Key System Parameters

The attitude control system is closed-loop system composed of the attitude sensing system, the control circuit, and the jet-powered execution mechanism on the satellite. The attitude motion is expressed in terms of the earth-centered orbit coordinate system and the satellite body coordinate system, as shown in Fig. 1. The angles between the two systems are called roll angle, pitch angle, and yaw angle and are denoted by ϕ, θ, ψ respectively.

1. Attitude Sensing System

In order to establish the earth-centered orbit coordinate system as a reference for attitude sensing and for bias measurement, and also to meet the requirements of eliminating initial attitude bias and establishing re-entry attitude, we have used an attitude sensing system which consists of two conical scan infrared horizon sensors and two two-degree-of freedom gyroscopes, as shown in Fig. 2. In designing the optical system and electronic circuit of the horizon sensor, measures were taken to improve the sensor performance. In particular, we took advantage of the complimentary characteristics between the infrared horizon sensor and the gyroscope: the gyroscope output has relatively small high-frequency noise but exhibits a constant drift, consequently it cannot be used as a long-term reference source; the infrared horizon sensor on the other hand is well suited as a long-term reference because of its small drift, but it has a high noise level and cannot serve as a reference for measuring attitude bias. By combining the merits of both sensing devices one can achieve an improved attitude sensing system.

Figure 1. Relationship Between Two Coordinate Systems
Earth Centered Orbit Coordinate System- OXYZ
Satellite Body Coordinate System - oxyz

key: 1. center of earth
2. satellite
3. orbit plane

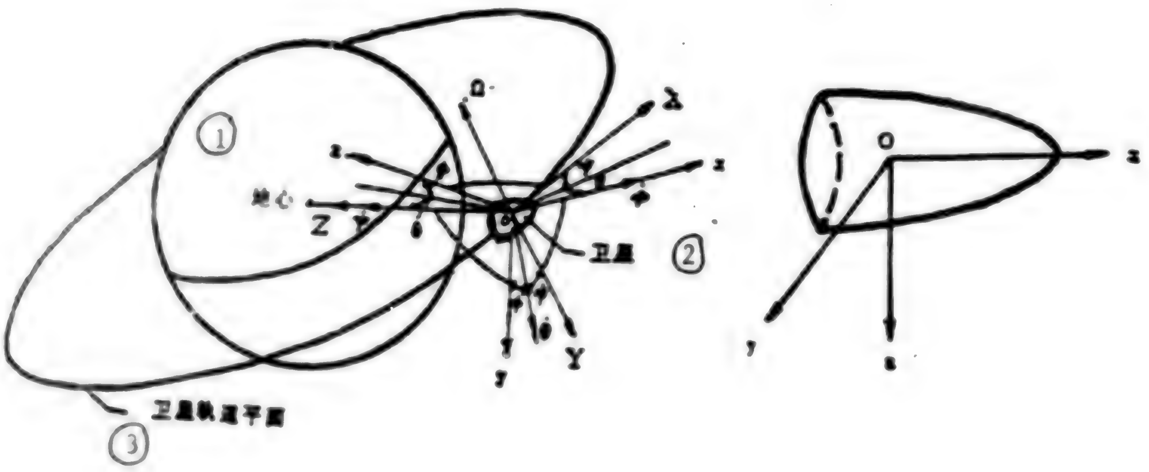

Figure 2. Composition of the Attitude Sensing System
⊙ - sensing device ◉ - torque device

key: 1. pitch angle signal
2. pitch infrared horizon sensor
3. amplification and correction
4. compensation signal
5. phase sensitive
6. large angle sensor
7. horizontal gyroscope
8. pitch axis sensing system

Figure 2 (continued)

9. programmed mechanism
10. pulse generator
11. roll axis
12. pitch axis
13. yaw axis
14. yaw angle signal
15. roll and yaw axes sensing system (gyrocompass)
16. vertical gyroscope
17. roll infrared horizon sensor
18. roll angle signal

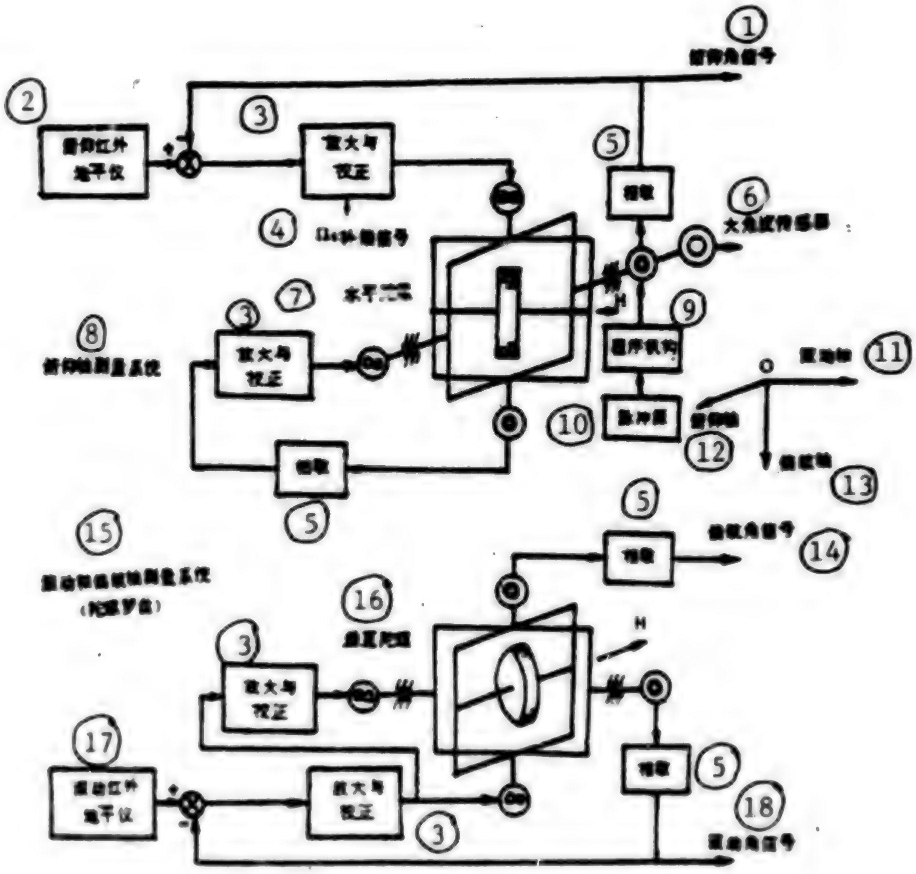

It can be seen from Fig 2 that the long-term sensing reference is provided by the infrared horizon sensor; the short-term or transient sensing reference is provided by the gyroscope, which also generates the relatively smooth attitude bias signals for all three channels. Specifically, the pitch bias signal is generated by the pitch infrared horizon sensor and the horizontal gyroscope; the yaw and roll bias signals are generated by the gyrocompass which consists of the roll infrared horizon sensor and the vertical gyroscope. The programmed mechanism located on the outer gimbal of the horizontal gyroscope is used to provide programmed bias signals during re-entry, and the large angle sensor is used to monitor the operation of the attitude control system during re-entry. During the phase of initial bias elimination and the re-entry phase, the infrared horizon sensor must be cut off from the sensing system so that the system is basically open-loop, with both gyroscopes operating in a free state. Fig 2 represents the operating condition of the sensing system during normal orbit phase.

When the orbit is near circular, the signal is sufficiently small to be operating in a linear region, and Fig 2 can be represented by a simplified block diagram, as shown in Fig 3. From Fig 3 the following equations can be written:

$$\frac{d}{dt}(\theta_G-\theta)=K_\theta(\theta_N-\theta_G)+\Omega_0-\Omega+D_2 \qquad (1)$$

$$\frac{d}{dt}(\psi_G-\psi)+\Omega(\phi_G-\phi)=K_\psi(\phi_N-\phi_G)+D_3 \qquad (2)$$

$$\frac{d}{dt}(\phi_G-\phi)-\Omega(\psi_G-\psi)=K_\phi(\phi_N-\phi_G)+D_1 \qquad (3)$$

where θ, ψ, and φ are respectively the pitch, yaw, and roll angle of the satellite. θ_G, ψ_G, and φ_G are respectively the pitch, yaw, and roll gimbal angle of the gyroscope. K_θ, K_ψ, and K_φ are the amplification factors of the gyroscope precession angle provided by the amplifier and the gyroscope torque device. D_1, D_2 and D_3 are the effective drift rates of the gyroscope along the roll, pitch, and yaw axes, which include gyroscopic drift, components of the precessional velocity of the orbital plane along the three axes, and second-order coupling effects, etc. Ω and Ω_0 are respectively the instantaneous and reference orbit angular velocities; the latter is provided by the amplifier.

Both Fig 3 and equations (1), (2), and (3) indicate that the key parameters here are K_θ, K_ψ, and K_ϕ. In principle they should be chosen to achieve a compromise between the noise level of the horizon sensor and the corresponding gyroscopic drift, so that the mean square value of attitude sensing error is minimized; also, the effect on gas consumption due to noise in the intermediate circuits should be considered. This is particularly important for lower orbit satellites whose infrared horizon sensors cannot operate in the ideal

14-16 micron band. In the design of this system, we selected the three parameters based on the following conditions: maximum gyroscope drift 4 degrees per hour, root mean square error in the horizon sensor 0.25 degrees, and stable noise whose bandwidth is equal to 1000 times the orbit angular velocity.

Figure 3 Simplified Block Diagram of the Attitude Sensing System

key: 1. pitch axis attitude sensing ayatem
2. gyrocompass system

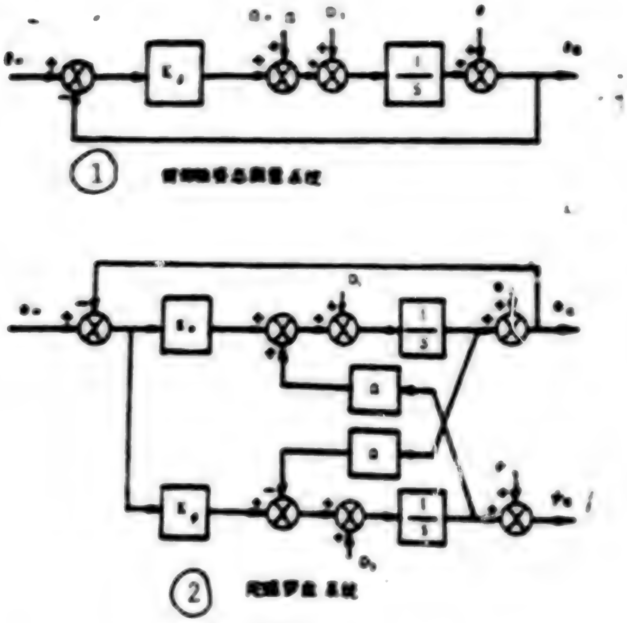

In addition, the following problems are also addressed in the design:

(1) Limiting the Maximum Precessional Velocity of the Gyroscope

In order to avoid increase in attitude bias and excessive gas consumption caused by the large output signal when the horizon scans toward the sun or the moon, the magnitudes of K_θ, K_ψ, and K_ϕ should be limited. In this design we impose the following limits:

gyroscope saturated precession velocity in the pitch axis ≤ 0.06 °/s
gyroscope saturated precession velocity in the yaw axis ≤ 0.054 °/s
gyroscope saturated precession velocity in the roll axis ≤ 0.018 °/s

(2) The Problem of Matching Transfer Coefficients Between the Infrared Horizon Sensor and the Gyroscope

During actual implementation, the transfer coefficient between the input angle and output voltage of the infrared horizon sensor, K_1, may differ from the transfer coefficient between the input angle and the tranducer output voltage of the gyroscope, K_g. Analysis and experiment show that when K_h and K_g are different, the system will operate on the limit cycle, resulting in increased gas consumption. This effect is particularly pronounced in the roll channel. For example, when K_h exceeds K_g by 10 %, stable "dual ejection phenomenon" will occur in the yaw-axis thrust system, and the angular velocity of the limit cycle and the gas consumption both increase by a factor of 2. In this design we impose the following requirements:

roll channel: $(K_h - K_g)/K_g \leqslant 6\%$
pitch and yaw channels: $(K_h - K_g)/K_g < 10\%$

(3) Selection of the Time Constant T_g for the Gyroscope Phase Sensitive Stage

Clearly, increasing T_g will reduce the damping of the system. If T_g reaches a certain value, the coordinated thrust operation of the system may be damaged. The dynamic characteristics of the pseudo-velocity gain feedback system require that T_g should be no larger than the charge constant T_{fc}. In general T_g should be less than 0.2 seconds.

(4) Time Constant of the Infrared Horizon Sensor T_h

Increasing T_h will cause an increase in the steady-state limit cycle velocity and gas consumption. Ideally T_h should be one order of magnitude smaller than the time constant of the tracking circuit. In general T_h should be less than 2 seconds.

2. Intermediate Control Circuit and Execution Mechanism

In order to achieve good system performance during three different phases of operation, an on-off type control and a cold-jet execution mechanism with two thrust levels were selected. This design was chosen primarily for its simplicity, reliability, light weight, and low power consumption. Fig 4 shows the block diagram of the pitch channel control system, and Fig 5 shows the composition of the execution mechanism.

Figure 4 Block Diagram of the Pitch Channel Attitude Control System
I = pitch axis moment of inertia
S = Laplace operator

key: 1. large thrust execution mechanism
2. perturbation
3. small thrust execution mechanism
4. attitude measurement

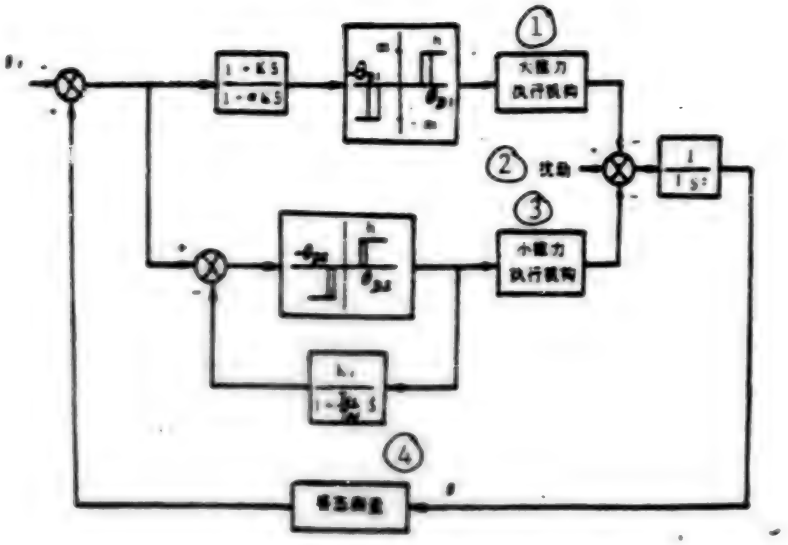

Fig 5 Composition Diagram of the Jet Execution Mechanism

key: 1. gas bottle
2. 210 atmosphere
3. pressure reduction valve
4. pressure regulator
5. solenoid control valve
6. pitch jet nozzle
7. yaw jet nozzle
8. roll jet nozzle

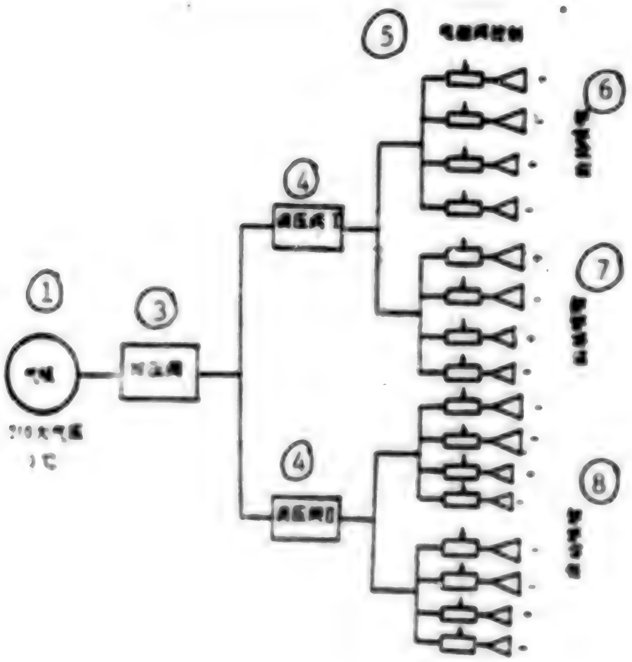

For convenience, the pitch channel is used to illustrate the large and small thrust systems, and the satellite pitch angle is approximated by the output gimbal angle of the horizontal gyroscope.

(1) Large Thrust Pre-correction System

The large thrust pre-correction system is primarily used to eliminate the initial attitude bias and to establish re-entry attitude. In order to increase system damping, a pre-correction circuit is used. The main design requirement for the large thrust system is to eliminate initial attitude bias and to establish re-entry attitude with a minimum amount of gas consumption in the shortest time possible.

It is clear from Fig 4 that if the dynamic effects of the execution mechanism and the time constant αK are neglected, the control response of the large thrust system can be described by the following equations:

$$m=-1,\ mA=-A,$$

$$\text{当}\quad \theta+\theta_p+K(\dot{\theta}+\dot{\theta}_p)\geqslant\theta_D \qquad (4)$$

$$m=+1,\ mA=+A,$$

$$\text{当}\quad \theta+\theta_p+K(\dot{\theta}+\dot{\theta}_p)\leqslant-\theta_D \qquad (5)$$

$$m=0,\ mA=0,\ \text{当}-(1-h)\theta_D\leqslant\theta+\theta_p+K(\dot{\theta}+\dot{\theta}_p)\leqslant(1-h)\theta_D \qquad (6)$$

$$\ddot{\theta}=A_d+mA=(M_d+mFl_i)/I \qquad (7)$$

Here θ_p and $\dot{\theta}_p$ are respectively the programmed turn angle and angular velocity during re-entry. A_d and A are respectively the angular acceleration produced by the perturbation torque M_d and the control torque $F l_j$. F is the thrust force and l_j is the moment arm. Clearly, during the initial bias elimination phase, both θ_p and $\dot{\theta}_p$ are zero. In actual implementation, equations (4)-(7) should be modified to account for the effects of the dynamics of the execution mechanism and the time constant αK. We shall now briefly discuss the problem of selecting the key parameters in the above equations.

i) selection of the parameter K of the pre-correction circuit

Under the simplified conditions described above, analytical or simulation methods can be used to determine graphically the variation of the transient process time T_t and the total impulse I_Σ as a function of the parameter K, as shown in Fig 6. T_t is the time required to eliminate a specified amount of initial bias. Given the specific impulse of a gas, one can compute the gas consumption Q based on the total impulse I_Σ. During the phase of re-entry attitude establishment, it refers to the time required to eliminate the remaining attitude bias and angular velocity after the pitch axis has made a turn of a specified angle θ_P. Fig 6 shows that when all other parameters are fixed, both T_t and I_Σ decrease with increasing K in a given range; but when K is greater than 4 seconds, T_t begins to increase. Therefore, the value $K \approx 4$ seconds is an appropriate choice.

Figure 6 Variation of the Transient Process Time T_t and total Impulse I_Σ with K

key: 1. transient process time T_t (seconds)
2. total impulse I_Σ (kg·seconds)
3. seconds

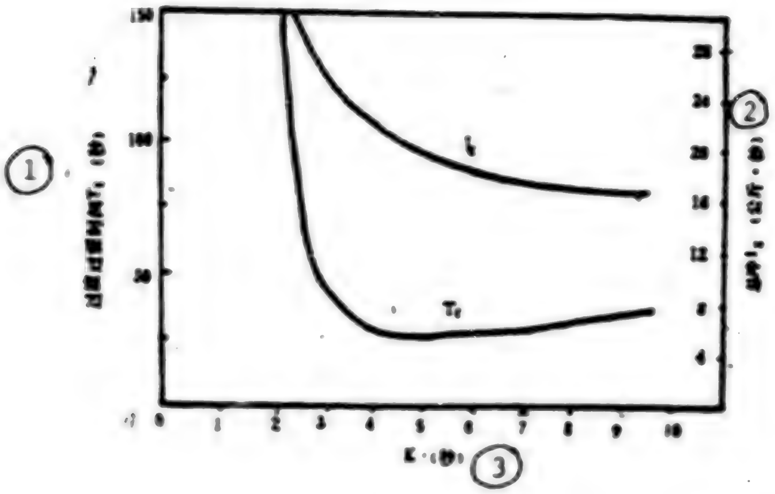

ii) selection of the switching dead zone θ_D and the damping cycle coefficient h

In order to conserve gas, the large thrust system is shut off whenever the attitude bias falls within ± 1°. Also, in order for the satellite pitch angle to reach $\theta_P \pm \varepsilon$ quickly (ε is the allowable error), the value of θ_D is chosen to be 1°. A large damping cycle coefficient h will improve noise suppression, but at the expense of system stability. A compromised value for h is h = 0.1.

iii) selection of the control angular acceleration A

The effects of A on T_t and I_Σ are shown in Fig 7 and Fig 8 respectively. It is seen that for K = 3-6 seconds, T_t and I_Σ no longer decrease with A when $A > 0.5\ {}^\circ/s^2$. When A is small, both T_t and I_Σ increase significantly. Therefore, $A = 0.5\ {}^\circ/s^2$ appears to be a good choice.

iv) selection of the programmed turn velocity

For simplicity, reliability, and ease of implementation, we selected a fixed turn velocity based on a compromise between T_R (time required to establish re-entry attitude) and gas consumption Q. Specifically, Q is minimized under the condition $T_R \leqslant 60$ seconds. In this design,

$\dot{\theta}_f$ is chosen to be $2.07\times10^{-2}\,\theta_f$ °/s.

Figure 7 Relationship Between Transient Process Time T_t and Control Angular Acceleration A

key: 1. seconds
     2. degrees per second squared

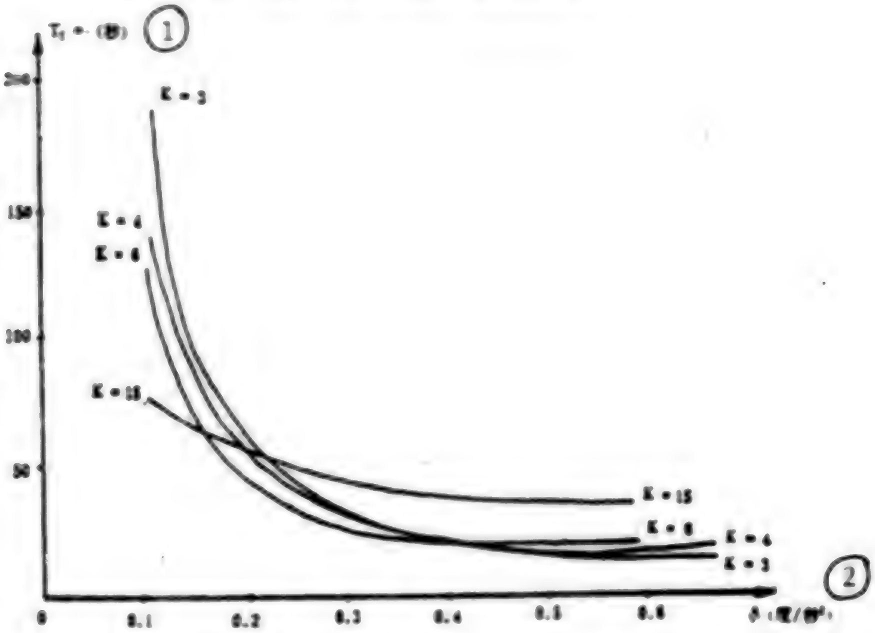

Figure 8 Relationship Between Total Impulse I_Σ and Control Angular Acceleration A

key: 1. kg·second
     2. degrees per second squared

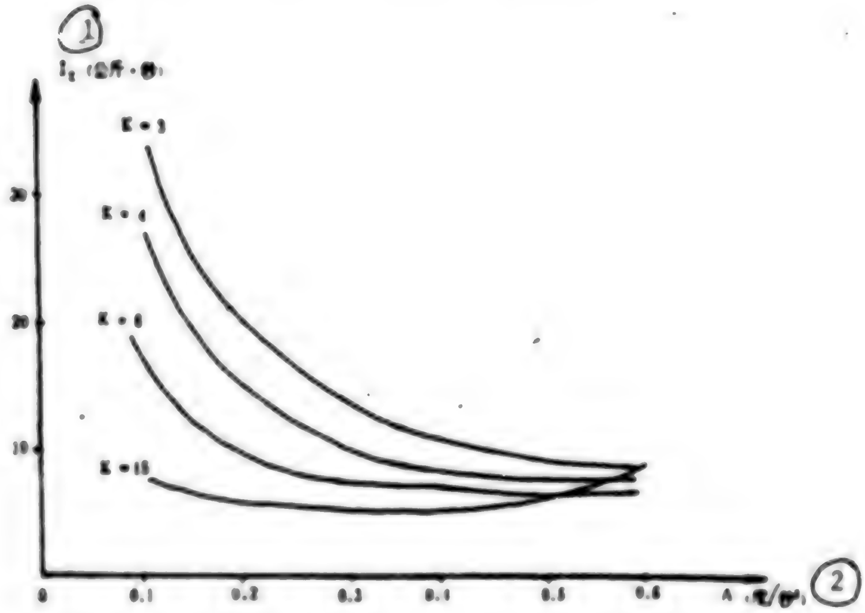

(2) Small Thrust System

The small thrust system is primarily used in the long-term orbit phase where high precision attitude control is required. In order to minimize gas consumption, to meet the precision requirements in attitude and angular velocity, and also to achieve good dynamic damping and long operating life, we used a pseudo-velocity gain feedback control system where the discharge time constant T_{fd} is larger than the charge time constant T_{fc}, as shown in Fig 4.

The pseudo-velocity gain feedback control system is a pulse modulation system. In the absence of perturbation torque, the system remains in the operating state of ideal limit cycle ① shown in Fig 9(A) (without special measure it is very difficult for the system to operate in the optimum state of limit cycle ③). The effective minimum thrust pulse width T_d of the system output is

$$T_d = T_{on} + \Delta T \qquad (8)$$

$$T_{on} = -T_{fc}\ln\left(1-\frac{h\theta_d}{K_f a}\right) \qquad (9)$$

$$\Delta T = (T_{pd}-T_{pr})+(T_{md}-T_{mr}) \qquad (10)$$

where T_{on} is the minimum pulse width of the pseudo-velocity gain controller, and ΔT is the increased pulse width after taking into account the thrust time delay, as given by equation (10). T_{pr} and T_{pd} are respectively the forward and backward time delays of the solenoid valve, T_{mr} and T_{md} are respectively the effective time constants of the forward and backward thrust. θ_d is the dead zone of the pseudo-velocity gain controller. In this case, the limit cycle angular velocity of the system is

$$\theta_R = \frac{a}{2}T_d = -\frac{aT_{fc}}{2}\ln\left(1-\frac{h\theta_d}{K_f a}\right)+\frac{a\Delta T}{2} \qquad (11)$$

Figure 9 Limit Cycle Operation of the Pseudo-Velocity Gain Feedback System

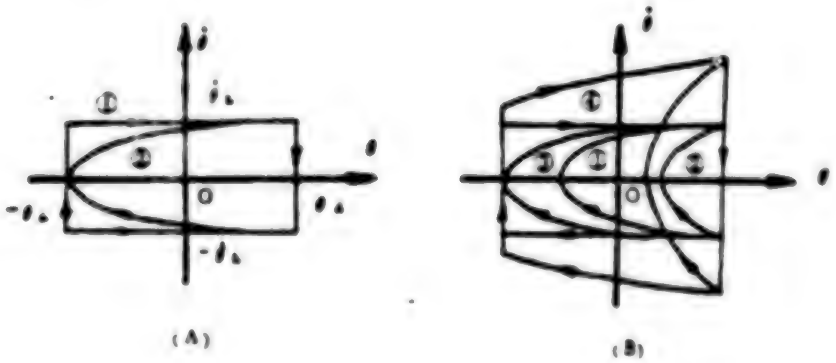

For a given set of structural parameters and fixed specific impulse of the jet gas, we can define the angular velocity increment per unit time, denoted by q, as the key factor affecting gas consumption. Then under the condition of ideal limit cycle operation with no perturbation torque,

$$q=\frac{2a}{T}T_d=\frac{\dot{\theta}_R^2}{\theta_d}=\frac{f^2l_1^2}{4J^2\theta_d}T_d^2 \tag{12}$$

Here a is the control angular acceleration produced by the small thrust force f, and T is the period of the limit cycle. It can be seen from equations (11) and (12) that in order to reduce $\dot{\theta}_R$ and q, T_d should be decreased, and ΔT should be made as small as possible. But in practice ΔT is generally greater than zero, hence T_d is in general larger than T_{on}.

When the system is subject to perturbation torque, it will be in an operating state denoted by the limit cycles ① and ② in Fig 9(B). Under most conditions it is difficult to be in the optimum state of limit cycle ③ . The curve ① represents the phase trajectory when the perturbation torque is less than the curve ② . Clearly, a small value of $\dot{\theta}_R$ will tend to form a one-sided jet. The larger the perturbation torque, the more frequently jet actions will take place. If the impulse torque ΔH_d on the satellite due to M_d is fixed, then in principle the gas expenditure required to overcome the perturbation torque is also fixed. If every jet action is used to overcome the perturbation torques, then the number of jet actions is given by:

$$\eta=\frac{\int M_d dt}{Fl_1T_d}=\frac{\Delta H_d}{Fl_1T_d} \tag{13}$$

It is clear from equation (13) that in the presence of perturbation torques, $\dot{\theta}_R$ or T_{on} should be properly increased in order to reduce the number of solenoid valve actions, and to prolong the life of the execution mechanism without increasing gas expenditure. It should be noted however that improper increase in T_{on} may result in the formation of two-sided jets (see curve ④ in Fig 9(B)) and reduced jet efficiency.

In the design of this system, the limit cycle velocity of the yaw channel, which has large perturbation torques, is chosen to be twice as large as that of the pitch channel or the roll channel which has smaller perturbation torques. A similar relation exists for the corresponding T_d. The selected values of $\dot{\theta}_R$ and T_d are summarized in Table 1.

Table 1 Selected Values for $\dot{\theta}_R$ and T_d

key: 1. parameter
2. channel
3. pitch and roll
4. yaw
5. limit cycle angular velocity $\dot{\theta}_R$
6. effective minimum thrust pulse width T_d

参 ① 数 ② 通 道	⑤ 极限环角速度 $\dot{\theta}_k$	⑥ 喷管的最小推力 脉冲宽度 T_d
③ 俯仰和滚动	$2.5\times10^{-}$[illegible] °/s	50ms
④ 偏 航	$5.0\times10^{-}$[illegible] °/s	100ms

Equation (11) shows that $\dot{\theta}_k$ is determined by a and T_d. The selection of θ_k and T_d clearly will involve the selection of a. In this design the value of a is chosen to be 0.1 °/s^2, which is much larger than the angular acceleration produced by perturbation torques. This choice of a can be easily implemented and it ensures the coordinated operation between large and small thrust forces.

Furthermore, the values of T_{on} and ΔT can be properly allocated based on analysis and experimental results. In this design the allocation of T_{on} and ΔT is shown in Table 2.

Table 2 Allocation Of T_{on} and ΔT

key: 1. parameter
2. channel
3. pitch and roll
4. yaw

参 ① 数 ② 通 道	T_{on}(ms)	ΔT(ms)
③ 俯仰和滚动	37	13
④ 偏 航	87	13

It is well known that in a pseudo-velocity gain feedback control system, when the attitude bias θ reaches a certain value θ_s, the system will be in a state of continuous jet action. The attitude bias which corresponds to the initiation of this state is called the "saturation jet angle," and is given by:

$$\theta_s = K_{p}a + (1-h)\theta_d \tag{14}$$

It is an important parameter in ensuring coordinated large and small thrust operation. In this design, θ_s is chosen to be 0.6° - 0.75°, which takes into account the value of 1° for the large thrust switching dead zone θ_D.

In addition, if the dynamic characteristics of the execution mechanism and the sensor system are ignored, the system can be roughly treated as a second order linear system with damping ξ and natural frequency ω_n, which are given by:

$$\zeta = \sqrt{\frac{T_{fc} T_{fd}}{4K_f}} \tag{15}$$

$$\omega_0 = \sqrt{\frac{T_{fc}}{T_{fd} K_f}} \tag{16}$$

Having presented the fundamental relations and data, we are now in a position to select some of the key parameters of the small thrust system.

i) selection of the switching characteristics

The dead zone θ_d should be matched with measurement error of the sensing system in order to meet the attitude precision requirement during the orbit phase. Furthermore, the dead zone of the small thrust system θ_d should be much smaller than that of the large thrust system θ_b to ensure that the primary operation during the orbit phase is provided by the small thrust system. We chose $\theta_d = 0.3°$.

The damping cycle coefficient h not only affects T_{on} but also affects the noise suppression capability of the system. Equation (9) shows that when all other parameters are fixed, the smaller h is, the smaller T_{on} becomes, and the weaker is the noise suppression capability. On the basis of simulation and experimental results, a compromised value of h is chosen to be 0.1.

ii) selection of the feedback circuit parameters

In order to ensure coordinated operation of the large and small thrust system, θ_s is chosen to be 0.7°; it follows from equation (4) that K_f = 4.3 seconds^2.

By requiring that the pulse width T_{on} is minimum, one can compute the charge time constant T_{fc} from equation (9).

In order to require large dynamic damping in the system, the discharge time constant T_{fd} can be determined from equation (15). In this design we chose $\zeta = 1$.

The selected values for T_{fc} and T_{fd} are shown in Table 3.

On the basis of the selected key parameter values, one can easily deduce requirements on the thrust level of the execution mechanism and its dynamic characteristics. The nominal values of the large and small thrust levels for each channel are presented in Table 4.

Table 3 Selected Values For T_{fc} and T_{fd}

key: 1. parameter
2. charge time constant
3. discharge time constant
4. channel
5. milliseconds
6. seconds
7. pitch and roll
8. yaw

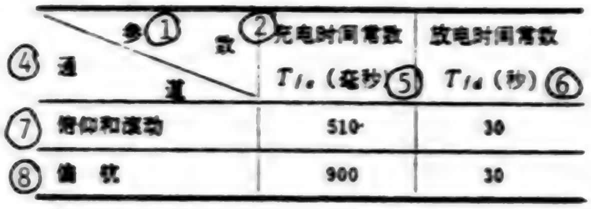

参① 数 ④ 通 道	② 充电时间常数 T_{fc}（毫秒）⑤	放电时间常数 T_{fd}（秒）⑥
⑦ 俯仰和滚动	510	30
⑧ 偏 航	900	30

Table 4 Nominal Thrust Values For Each Channel

key: 1. type
2. large thrust (g)
3. small thrust (g)
4. channel
5. pitch
6. yaw
7. roll

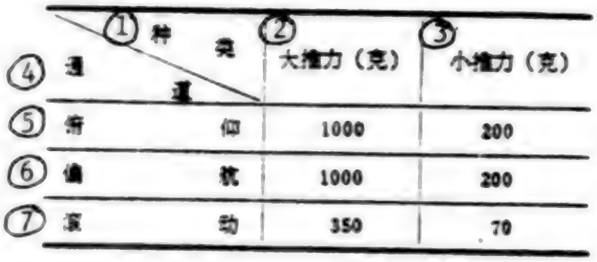

① 种 类 ④ 通 道	② 大推力（克）	③ 小推力（克）
⑤ 俯 仰	1000	200
⑥ 偏 航	1000	200
⑦ 滚 动	350	70

During the initial design of the system, a large number of mathematical simulations were performed. After the first prototype was developed, the system design was verified using semi-empirical and empirical methods; furthermore, studies were conducted on the coordinated operation of large and small thrust system for each channel and the coupling effects between the three axes. On the basis of these results regular product development was initiated, and interface requirements with respect to the overall system and other subsystems were established. To meet the reliability requirement in space, a large amount of analyses and experimental work were performed during regular product development. However, due to limited space they will not be discussed here.

III Flight Test Results

In order to monitor the performance of the attitude control system during flight and to obtain useful data, important parameters are measured using the telemetry system; in addition, a star camera is also installed in the satellite for monitoring the attitude control system. Based on data collected during three flight tests, the performance of the attitude control system under three different phases of operation and preliminary analysis results are reported below.

1. Phase 1 - Elimination of Initial Attitude Bias

Telemetry data indicate that among the three satellites, the first satellite had relatively poor initial attitude bias; the two subsequent satellites showed significant improvement. The initial attitude bias of the first satellite is shown in Table 5, and the dynamic process of eliminating initial bias is shown in Fig 10.

Table 5 Initial Attitude Bias of the First Satellite

key: 1. attitude bias
2. initial bias angle (degree)
3. initial angular velocity (degrees/second)
4. channel
5. pitch
6. yaw
7. roll

④ 通道 \ 姿态偏差 ①	② 初始姿态偏差角（度）	③ 初始姿态角速度（度/秒）
⑤ 俯仰	+1.13°	−2.24
⑥ 偏航	+1.68	+0.17
⑦ 滚动	+0.38	−0.17

Figure 10 Dynamic Process of Initial Bias Elimination for the First Satellite (from gyroscope telemetry data)

key: 1. pitch angle (degrees)
2. yaw angle (degrees)
3. roll angle (degrees)
4. time (seconds)

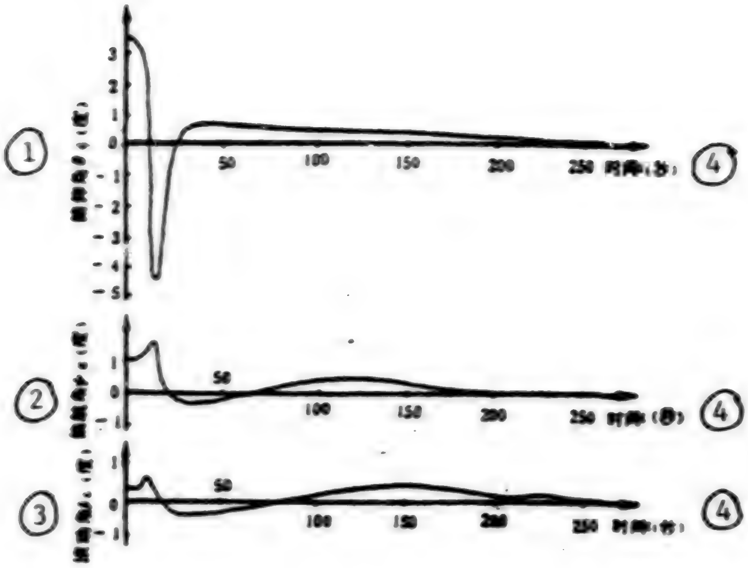

The performance of the attitude control system during this phase can be seen from Table 6. In summary, the operation of the system during the initial bias elimination phase is quite normal; the results are in good agreement with theoretical analysis, and show that the system is well capable of capturing the initial attitude.

Table 6

key: 1. content
2. maximum overshoot or point of interest
3. time required to achieve ± 0.7°
4. satellite
5. degrees
6. seconds
7. monotonically decreasing

④ 内 ① 容 卫 星	② 最大超调角或过程特点	③ 进入±0.7°的时间
Ⅰ	−5.36度 ⑤	12秒 ⑥
Ⅱ	⑦ 单调衰减	12秒 ⑥
Ⅲ	⑦ 单调衰减	6秒 ⑥

2. Phase 2 - Orbit

(1) Precision of Attitude Control

The actual precision of the attitude control system was obtained from data taken by the star camera. From a photograph of the stars, one first obtains the satellite attitude with respect to an earth-centered celestial coordinate system, then from orbit data it can be converted to attitude with respect to an earth-centered orbit coordinate system. The precision of the satellite attitude derived from star camera data is quite high. Typical attitude data are shown in Fig 11. The actually achieved biases in attitude angle and angular velocity are shown in Table 7.

Table 7 Actually Achieved Attitude Bias

key: 1. content
2. bias in attitude angle (degrees)
3. bias in angular velocity (degrees/second)
4. channel
5. pitch
6. roll
7. yaw

① 内容 ④ 通道	② 姿态角偏差（度）	③ 姿态角速度偏差（度/秒）
⑤ 俯仰	≤0.7	≤0.01
⑥ 滚动	≤0.7	≤0.02
⑦ 偏航	≤1.5	≤0.02

Figure 11 Typical Attitude Data Taken By Star Camera

key: 1. roll (degrees)
2. pitch (degrees)
3. yaw (degrees)
4. time (seconds)

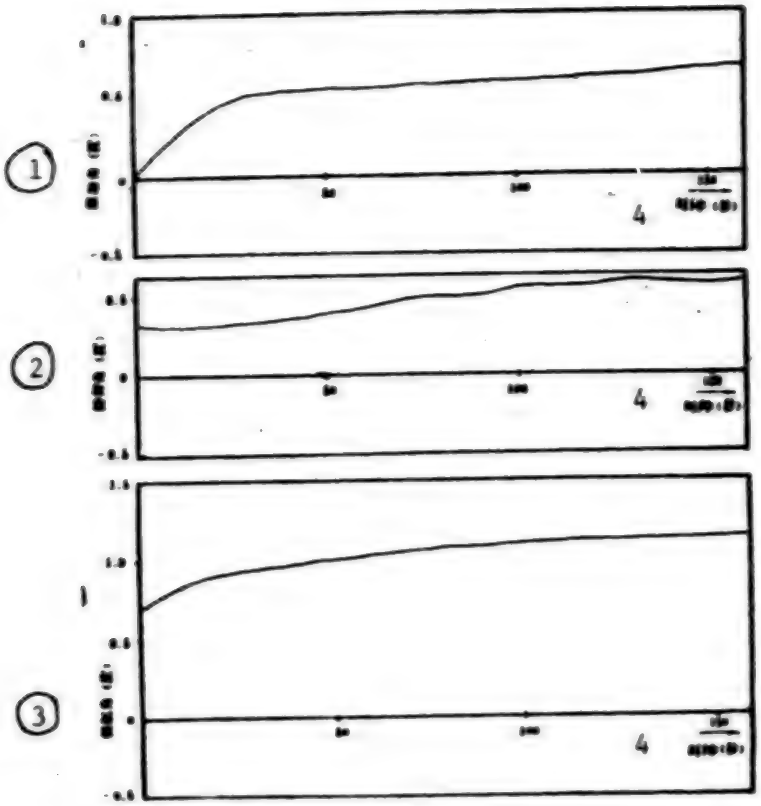

(2) Noise Spectral Density in the Infrared Horizon Sensor

On the basis of telemetry data of the infrared horizon sensor and the gimbal angle of the gyroscope during the orbit phase, a preliminary analysis was made of the output noise from the horizon sensor. In the analysis it is assumed that the noise is generated by a steady-state random process. By using Fourier transforms one can compute the power spectral density of the output noise. After making dynamic corrections to the sensor system using the method of Ref 4, we determined the bandwidth of noise spectral density to approximately 12 times the orbit angular velocity. However, due to the limited amount of continuous data, this result should be regarded only as preliminary.

3. Phase 3 - Establishment of Re-entry Attitude

During this phase, the performance of the attitude control system in all three satellites was essentially the same. A typical performance curve is shown in Fig 12, which represents the entire dynamic process of the attitude control system of the third satellite. From Fig 12 the following observations can be made:

(1) the large angle sensor output of the horizontal gyroscope outer gimbal indicates that the satellite rotated an angle θ_r in the negative pitch direction; its dynamic process was in complete agreement with theoretical analysis.

(2) the small angle sensor output of the horizontal gyroscope outer gimbal indicates that at the beginning of attitude adjustment, the output rose rapidly in the positive direction, reaching the maximum overshoot angle; after a certain time T_p, the output becomes almost zero. One can deduce from this process that the programmed mechanism actually rotated an angle θ_p in the pre-determined direction at a pre-determined angular velocity $\dot{\theta}_p$, and the satellite also reached this angular velocity. Eventually, the satellite stabilized in the range $\theta_p \pm \varepsilon$. The entire attitude adjustment process took approximately 55 seconds.

The above results indicate that the process during the re-entry phase was basically as predicted, and the system operation was completely normal.

Figure 12 Typical Performance During the Re-entry Phase (obtained from gyroscope telemetry data)

key: 1. large angle sensor output of the horizontal gyroscope
2. command time
3. seconds
4. small angle sensor output of the horizontal gyroscope

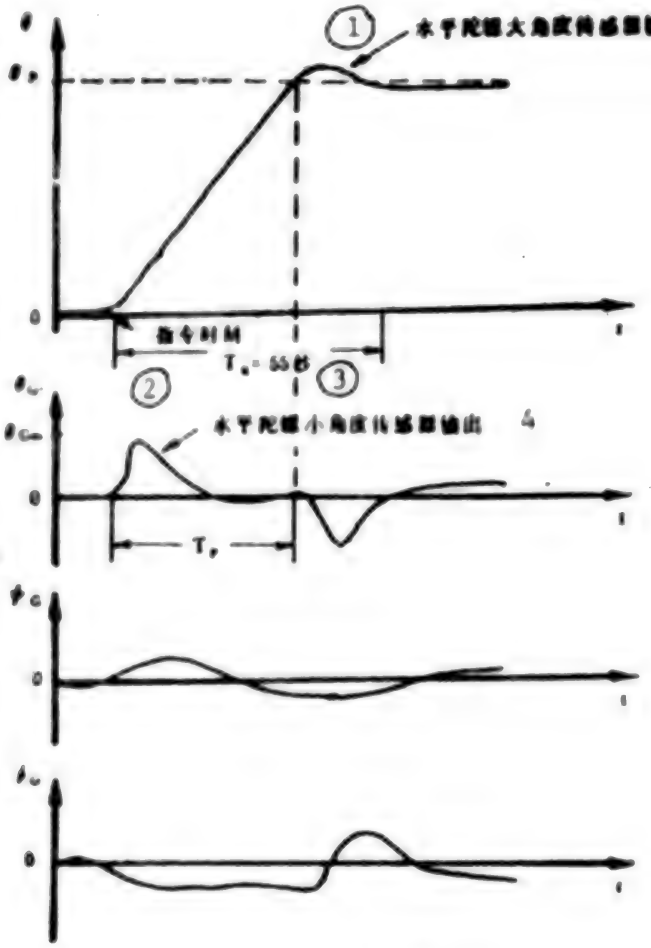

4. Gas Consumption of the Attitude Control System

Results from the three flight tests indicate that the gas consumption of the attitude control system (either theoretical or actual consumption) successively decreased. In particular, the gas consumption of the third satellite was decreased by a factor of two compared to the first satellite. The main reasons for the reduction are as follows:

(1) Based on the first two flight tests, improvements were made in the system parameters of the third satellite, particularly in the key parameters of the sensor system. As a result, the noise suppression capability was increased, leading to lower gas consumption.

(2) A cut-off filter was installed in the optical system of the infrared horizon sensor, thereby reducing the effects of the sun, moon, and cloud on the output of the horizon sensor, and leading to lower gas consumption.

IV Conclusion

Results from the three flight tests have validated the design of the first-generation attitude control system of China's recoverable earth-orienting technology testing satellite. The operation of the system was shown to be reliable and normal. In particular, improvements in the third satellite were proven very effective, and its mission was successfully completed. Useful data and valuable experience were collected to provide a foundation for developing similar attitude control systems in the future.

For future efforts, we should improve the precision of the attitude control system, particularly in the yaw axis. In addition, we should apply system engineering and modern control theory to the design and development of attitude control systems to extend the operating life of the satellite and to reduce development cost.

3012
CSO: 8111/1472

BRIEFS

LARGE CAPACITY DESALINATION COMPLEX--Correspondent Chen Xiuchang reports: Recently, PRC's first electrodialysis seawater desalination apparatus with a daily output of 200 metric tons went into production in the Xisha Islands. At present, this is the largest equipment of this kind in the PRC. This seawater desalination apparatus has certain advanced characteristics and is economically sound. Its power consumption is relatively low. It is easy to operate and is equipped with automatic monitoring and alarm systems. The quality of the desalinated water not only meets with state regulations on water quality standards but is even better than the quality of drinking water in large cities such as Beijing, Tianjin and Shanghai. Its production cost is only 1/5 of the cost of shipping water in by boat. This seawater desalination apparatus was built by the State Maritime Bureau Oceanography Institute No 2 with assistance from the East China Chemical Engineering Institute, the Military Medical College No 2 of the Chinese People's Liberation Army, the Nanhai (South China Sea) Fleet and the Meishan Saltworks in Ningbo, Zhejiang. The apparatus passed on-site technical assessment in early July. [Text] [Beijing GUANGMING RIBAO in Chinese 24 Jul 81 p 1]

CSO: 4008/451

Cement Production

AUTHOR: YANG Dahua [2799 1129 5478]

ORG: Senior Engineer

TITLE: "Results and Understandings of the Reconstructed Vertical Kiln of Tangshan Municipal Cement Plant"

SOURCE: Beijing SHUINI [CEMENT] in Chinese No 7, 81 pp 17-20

ABSTRACT: The Tangshan Municipal Cement Plant was built in 1958. Before its reconstruction in 1974, it had 2 semi-mechanized vertical kilns. They produced, in 1973, 39,221 tons of clinkers and 70,573 tons of No 400 slag cement. When the material was unloaded from the kiln, there was a great deal of dust; therefore, the city invested 120,000 yuan to reconstruct a mechanized vertical kiln in the original plant to replace the original two. The plant designed and made the equipment and installed it under the guidance of specialists sent by the Cement Designing Academy. The reconstructed kiln has been operating very well, in spite of the earthquake. The annual turn-over rate is as high as 86.1 percent. The shop is now operated by 14 workers instead of the original 27. The paper introduces briefly the reconstruction design and the improvements over the original kilns. Drawings depicting the original kiln and the reconstructed one are included.

AUTHOR: None

ORG: Chatou Cement Plant, Guangzhou City

TITLE: "Φ4 Nodule-forming Tray Equipped With an Automatic Scraper"

SOURCE: Beijing SHUINI [CEMENT] in Chinese No 7, 81 pp 28-29, 9

ABSTRACT: Just like nodule-forming trays of vertical kilns of other cement plants, the Φ nodule-forming tray of the Chatou Cement Plant had the problem of being sticky. An automatic scraper was designed and installed on the tray. It includes a scraper blade and a handle, a gliding track and wheels, an electric motor, a decelerating device, and rollers. The automatic scraper can remove material accumulated on the bottom of the tray but it cannot remove the material adhering to the edges of the tray. In Chatou Cement Plant, measures were adopted to control the moisture of the nodule-forming tray when the automatic scraper was installed. These measures definitely improved the quality of the nodules, reduced labor intensity, and minimized the problem of sticky trays.

6168
CSO: 4009/432

Construction

AUTHOR: None

ORG: None

TITLE: "Important Speech Delivered by Vice Premier WAN Li [8001 6849] at the Award Meeting of Beijing, Tianjin, and Tangshan Engineering Competition"

SOURCE: Beijing JIANZHU [BUILDING CONSTRUCTION] in Chinese No 6, 30 Jun 81 p 1

ABSTRACT: An award meeting of Beijing, Tianjin, and Tangshan engineering competition, co-sponsored by the National Basic Construction Committee, the Chinese National Workers' Association, the National Bureau of Construction Engineering, the National Bureau of Labor, and the China People's Construction Bank, was held on 23 May in Beijing to present awards to 75 units for their various contributions to the 3 cities. At the award ceremony, Vice Premier Wan Li congratulated and thanked the recipients and pointed out the importance of constructing the capital into a beautiful city, Tianjin into an economic center of North China, and Tangshan from the earthquake damages. He also pointed out that in Handan City, the production value of each person averages 11,000 yuan and the average area of completed construction is close to 60 m^2/year. If all departments of construction of the country could reach that level, the goals of 4-modernizations would be reached much sooner. He encouraged all present at the meeting to summarize the experience of the past 30 years to continue in the spirit of diligent struggle for the service of the people and the users.

AUTHOR: GU Yicheng [7357 3015 2052]

ORG: None

TITLE: "Technique of Controlled Demolition of a Reinforced Concrete Building Framework in the City"

SOURCE: Beijing JIANZHU [BUILDING CONSTRUCTION] in Chinese No 6, 30 Jun 81 p 17

ABSTRACT: On 12 May, the technique of contolled demolition was successfully applied to remove a reinforced concrete framework in a busy section of Beijing. The framework included 24 reinforced concrete pillars of a height of 12.24m and 72 horizontal beams also of reinforced concrete. The structure was 42 m from the street and less than 10 m from the office of the work site. For the controlled demolition, 324 holes were drilled and a total of 21.75 kg of explosives were used. The space between the explosions was 75 milliseconds. The safety of the surrounding area was completely guaranteed. The paper includes a photo of the structure before it was demolished, but gives no clue as to the reason for the need of demolishing it.

AUTHOR: ZHANG Binggen [1728 3521 2704]
HUANG Lizhen [7806 0536 6297]

ORG: None

TITLE: "New Type of Side Pressure Meter"

SOURCE: Beijing JIANZHU [BUILDING CONSTRUCTION] in Chinese No 6, 30 Jun 81 p 31

ABSTRACT: The Changzhou Municipal Construction Designing Office of Jiangsu Province and the Liyang County Light Industry Machinery Plant successfully made the PY-1 and PY-2 side pressure meters. Since their applications in Oct 79, very good results have been obtained. The State's General Bureau of Construction and related organizations certified the 2 instruments to be of good property in Jul 80. These are special instruments used in the bore holes during engineering geological prospecting to determine such mechanical indices as the permissible load of the foundation, the modulus of deformation, etc. These indices are important parameters in designing the foundation of a building. The PY-1 side pressure meter is for manual compression. Compressed nitrogen pressure regulating valve is added to the manual compression operation for PY-2. Both of them are light and portable and produce accurate data with a quick test. A photo depicting one of these is included in the paper.

6168
CSO: 4009/429

AUTHOR: CHEN Yixiong [7115 0110 7160]

ORG: Liaoning Generating Plant

TITLE:: "Incremental Cost Scheduling and Economic Scheduling of Fossil-Fired Power Plant Loads"

SOURCE: Beijing DIANLI JISHU [ELECTRIC POWER] in Chinese No 6, 5 Jun 81 pp 11-14, 10

ABSTRACT: Incremental-cost scheduling involves distributing electrical load among generators in accordance with their operating economy. The procedure for constructing incremental cost load scheduling curves is described. Economic load scheduling has somewhat broader applicability, since in addition to distribution of load among generating units it also involves the following considerations: (1) the possibility of dealing with fluctuations in load economically by shutting down or starting up individual generating units; (2) determining which units should be shut down and in what manner to produce the most economical effect; (3) decision between a complete shutdown of a unit or operation on zero load with a small quantity of steam in the phase regulating or electric motor mode; (4) determination whether to use fixed voltage or variable voltage load decrease. The mathematical formulas involved in these calculations are presented.

AUTHORS: DING Wei [0002 0251], GUO Weimin [6751 0251 3046]

ORG: Baotou No 1 Heat and Power Plant

TITLE: "Improvements to Power Station Boiler Unit Gas Burners for Use with Blast Furnace Flue Gas"

SOURCE: Beijing DIANLI JISHU [ELECTRIC POWER] in Chinese No 6, 5 Jun 81 pp 18-20

ABSTRACT: Use of an on-site power station to burn blast furnace flue gas is beneficial in terms of both energy conservation and environmental protection. The Baotou No 1 Heat and Power Plant has five boilers, all 1950's Soviet models: Nos 1 to 3 are model TP-16 and Nos 4 and 5 are model PK-10, all with a capacity of 220 tons per hour. The TP-16 were already equipped with flue gas burners, but the design was ineffective, and accordingly the burner had not been used. The old burner was replaced by a new conical burner. The PK-10 was not equipped with a flue gas burner, and accordingly the improved burner design developed for the TP-16 was installed in these boilers as well. The results were increased operating stability, long service life and a saving on oil used for ignition and for combustion support at low loads.

AUTHOR: SONG Guobing [1345 0948 4426]

ORG: General Office of Electric Power Construction

SOURCE: Beijing DIANLI JISHU [ELECTRIC POWER] in Chinese No 6, 5 June 81 pp 32-38, 54

TITLE: "Discussion of Several Problems in Organization and Design of Fossil-Fired Power Plant Projects"

ABSTRACT: Techniques of organizing and planning the construction of fossil-fired power plants have advanced considerably throughout the world, and accordingly the General Office of Electric Power Construction is revising the 1964 "Construction Organization and Design Guidelines". Several problems involved in this revision are discussed. General procedures developed in the Soviet Union and Japan for coordinating the planning and design process are surveyed and a new tentative approach suggested. The effect of larger individual unit capacities on construction project organization is analyzed. Projects in different areas of China involving the same installed capacities have entailed different costs and levels of work, and factors which may lead to this divergence are discussed. Methods for drawing up comprehensive work schedules are considered, and a computer program developed by the Tongji University for the purpose, the "Model 719 Network Chart Calculation Program," is described. The importance of scientific organization of the construction process is noted, a formula for calculating peak manpower requirements is given, and ways of improving the design of construction site temporary structures are surveyed.

AUTHORS: CHEN Yili [7115 0110 3810], XU Deyu [6079 1795 5280], LI Jianguo [2621 1696 0948]

ORG: CHEN of Anhui Office of Electric Power, XU of Anhui Electric Power Experimental Research Institute, LI of Hefei Generating Plant

TITLE: "Experimental Investigation of Direct Ignition of Pulverized Coal with a High-Energy Arc"

SOURCE: Beijing DIANLI JISHU [ELECTRIC POWER] in Chinese No 6, 5 Jun 81 pp 52-54

ABSTRACT: Tests have been conducted using a high-energy electric arc for direct ignition of pulverized coal. The arc design includes a plasma arc initiator. A flow chart of the test facility is given. The variables tested in the experiments were: different varieties of coal, density of coal-air mixture, minimum power required for ignition, and procedure for continuing coal feed after the arc is turned off. It was found that the arc method could be successfully used for coal ignition, saving ignition oil, and that successful ignition was possible in a range of coal densities below 3.46 kg of pulverized coal per kilogram of air. Tables and graphs of experimental results are given.

8480
CSO: 4009/331

AUTHOR: WANG Maolin [3769 5399 2651]

ORG: Health and Technology Department, Anyang District Bureau of Electrical Power

TITLE: "Analysis of Rural Electrical Accidents in Anyang District of Henan"

SOURCE: Shanghai DIANSHIJIE [ELECTRICAL WORLD] in Chinese No 6, 81 p 18

ABSTRACT: From 1969 to 1979, 1108 persons died from electrical accidents in the district. In these 11 years, 289 persons died in the year of 1971 alone. These accidents served as warning signals for the management departments of electrical power of all levels. The electrical voltages, the age, gender, and occupation of the victims, the season of occurrence of the accidents (57.9 percent occurred in the 4 months from Jun to Sep) are summarized. The causes of the accidents are stated in the paper to be 40 problems belonging to 5 categories: (1) Various connections not conforming to standards; (2) Lack of maintenance and repair; (3) Working or touching live wire; (4) Hand touching electrified things, including clothing hanging on power line to dry, leaking light bulb, and the body of an electrocuted victim, etc.; (5) Privately connecting a wire to steal power, to use electricity to catch fish, or to repair electrical equipment without permission. Safety measures, aiming at overcoming these problems and preventing such accidents,are listed.

AUTHOR: (1) ZHU Gelin [6175 5514 2651]
(2) YAO Guanghui [1202 0342 6540]
(3) ZHANG Haigen [1728 3189 2704]

ORG: None

TITLE: "Brief News in Electrical Engineering"

SOURCE: Shanghai DIANSHIJIE [ELECTRICAL WORLD] in Chinese No 6, 81 p 19

ABSTRACT: This paper includes 3 short items, contributed by each of the authors: (1) A metrix type combination program control device made by Shanghai Electrical Meter Plant No 3 has been certified as TCF-510 program control device in Dec 80. It may be used for automatic regulation and control of the coal distribution system, pulverizing system, water treatment system, etc. of a power plant. (2) Silicon controlled low frequency device made by Shanghai Switch Plant No 2, with the help of Shanghai Industrial University, Chongqing Steel and Iron Designing Academy et al, for Shengli Oil Pipeline Plant. The device has a specified power of 50 kw and an output frequency of 16.7 Hz. (3)Two types of heating element economizing on electricity have been made by Shanghai Electrical Heating Apparatus Plant. The existing far infrared heating elements commonly used by industries have the shortcomings of large heat inertia and insensitive temperature control. About 20 percent of power may be saved with the 2 new types. They have been certified in Dec 80 and will be produced in batches in the coming year.

6168
CSO: 4009/436

AUTHOR: GAO Peiyong [7559 3099 3057]
ZHANG Qinglin [1728 3237 2651]
LI Xiliang [2621 1585 0081]

ORG: All of Office No 4, Research Institute of Radiology, Chinese People's Liberation Army Military Academy of Medicine

TITLE: "Comparative Studies of Dose-effects on in vitro Culture Human Blood to Induce Chromosome Aberrations by Irradiation of 60kV, 180kV, and 10MV X-rays"

SOURCE: Beijing YICHUAN [HEREDITAS] in Chinese No 4, Jul 81 pp 1-4

ABSTRACT: X-ray is the radioactive ray best understood and most frequently applied by mankind and whenever the biological effects of a new type of radiation are studied x-ray is always used to compare. In studies on chromosome aberration induction of various types of radiation, a large quantity of experimental data of γray, neutrons, electrons, and other particles have alreay been compared with those of x-ray. before such comparisons are relevant, chromosome aberration effects of x-ray of different doses should first be thoroughly understood, however. This is the objective of the experiment reported in the paper. The doses of 60kV, 180kV and 10MV, which are the most commonly applied doses in clinical diagnosis and treatment at present, are compared for their dose-effects on human blood chromosome aberration induction. Extracorporeal human blood, 36 specimens, are used for comparison and the rates of induced mutant cells are computed and compared.

AUTHOR: ZHAO Renjun [6392 0086 0193]
ZHANG Yifen [1728 4135 2780]
ZHENG Youxia [6774 1635 7209]

ORG: All of Shanghai Research Institute of Plant Physiology, Chinese Academy of Sciences

TITLE: "Studies on Mutagenesis of Auxotrophic Mutants of Streptomyces qingfengmyceticus by NTG"

SOURCE: Beijing YICHUAN [HEREDITAS] in Chinese No 4, Jul 81 pp 6-8

ABSTRACT: For the purpose of preparing experimental materials for genetic research on Streptomyces qingfengmycetius, the authors used NTG, a mutagenic chemical of obvious effects, to treat the microorganism and to select various auxotrophic mutants of various hereditary labels. The distribution and the mutation mechanism of these mutant types are analyzed. The experiment uses the M15 strain of Streptomyces qingfengmyceticus, a high productivity mutant obtained from a wild strain through a series of mutagenic treatments, and the Q-100, obtained from treating a wild strain with high temperature to cause it to become a mutant, having lost its ability to synthesize qingfengmycin. Characteristics of the auxotrophic mutants obtained by NTG induction are identified, analyzed, and discussed.

AUTHOR: WU Zhenchang [0702 2182 0235]

ORG: Hangzhou Pharmaceutical Plant No 2

TITLE: "Effect of Induction With 5-Fluoroureacil or Lithium Chloride on High Producing Mutant Streptomyces rimosus 1626 Derived From Fast Neutrons Radiation"

SOURCE: Beijing YICHUAN [HEREDITAS] in Chinese No 4, Jul 81 pp 9-10

ABSTRACT: In the course of a project involving compound treatment of Streptomyces rimosus with fast neutron and lithium chloride (WEISHENGWUXUE TONGBAO No 3, 1977 pp 27-29)the author obtained a strain of high producing fast neutron induced mutant S.rimosus 1626. For the purpose of further improving the antibiotic production of this strain of mutant, an experiment is carried out to compare the mutagenic induction action of 5-fluroureacil and lithium chloride. Results demonstrate that with 10 μg/ml of 5-fluoroureacil, the positive mutation rate is 35.9 percent; with 1 percent lithium chloride, it is only 11.4 percent. Compared with the untreated 1626 strain, the positive mutation rate through natural isolation is 22.9 percent, with a frequency of 6.5 percent in the range of productivity of 105-110 percent. If the oxytetracycline productivity rate is targeted at above 110 percent, mutants of such a productivity may be obtained only through 5-fluoroureacil treatment, at a rate of 1.3 percent.

6248
CSO: 4009/438

AUTHOR: XIAO Youfu [5135 0645 5346]

ORG: Research Institute of Sonics, Chinese Academy of Sciences

TITLE: "Lipote (White Dolphin) Qiqi and Its Sound"

SOURCE: Beijing XIANDAIHUA [MODERNIZATION] in Chinese Vol 3 No 7, 16 Jul 81 pp 2-3

ABSTRACT: Last year, the Wuhan Research Institute of Marine Biology, Chinese Academy of Sciences captured a live white dolphin and named it Qiqi. The white dolphin was mentioned in ERYA, a book of Han Dynasty (more than 2,000 years ago.) In Jin Dynasty [265-420 A.D.] GUO Pu [6751 3877] in his commentary on ERYA, gave the white dolphin a more detailed description. This paper briefly describes the historical record in China and the modern biological classification of this rare mammal. At present, these white dolphins reside only in the middle and lower reaches of Changjiang [Yangzi River.] Aside from describing such properties as being a fast swimmer, etc. the paper emphasizes the obvious degeneration of vision and the extremely well developed ears. A white dolphin sends out sonar signals through its nasal passage and uses the reflection wave to determine the distance, the size, and the nature of the target. The sonic signals of the white dolphin may be divided into 2 kinds: the long signal, lasting about half a second, at a frequency of about 6 kHz, are clearly audible to humans. The other is short, lasting 10-20 μsec only, and in a short chain of sonic pulses, which the author believes to be reply signals. These and other observations of the dolphin are discussed.

AUTHOR: YUAN Jizeng [0626 4949 1073]

ORG: Tianjin Research Institute of Fire Control Science, Ministry of Public Safety

TITLE: "Raging Fire of an Oil Tank"

SOURCE: Beijing XIANDAIHUA [MODERNIZATION] in Chinese Vol 3 No 7, 16 Jul 81 pp 36-37

ABSTRACT: At 9:45 in the night of 12 Sep 79, 2 oil pump workers were on night watch in a certain plant. One of them went to the oil tank to check the oil supply condition. There was no light. He flicked his cigarette-lighter for a peek. Instantly, an explosion was heard. The top of the oil tank was blown sky-ward and followed by a raging fire. The tank had a capacity of $4,000m^3$ with half of the tank buried below the ground surface. It contained crude oil. The oil spilled out in the explosion and every stream of oil was like a snake of fire attacking everywhere . All the firemen could do was to cool off the nearby tanks to prevent them from catching fire. At 12:00 midnight, suddenly the burning tank produced a large quantity of vapor and oil bubbles, which boiled over and caused everything to be engulfed, including 2 other oil tanks, 14 fire engines, and the entire plant. The fire kept burning for 14 hours. More than 10 persons were killed and the loss of property was estimated at several million yuan. This fire demonstrated the urgent need of developing techniques for controlling this type of explosive fires. Several automatic fire extinguishing devices and techniques are briefly described.

6168
CSO: 4009/428

END

END OF FICHE

DATE FILMED

31 Aug. 1981